

Circularly polarized colour reflection from helicoidal structures in the beetle *Plusiotis boucardi*

This content has been downloaded from IOPscience. Please scroll down to see the full text.

2007 New J. Phys. 9 99

(<http://iopscience.iop.org/1367-2630/9/4/099>)

View [the table of contents for this issue](#), or go to the [journal homepage](#) for more

Download details:

IP Address: 137.222.248.184

This content was downloaded on 23/12/2013 at 12:26

Please note that [terms and conditions apply](#).

## Circularly polarized colour reflection from helicoidal structures in the beetle *Plusiotis boucardi*

S A Jewell<sup>1,3</sup>, P Vukusic<sup>1</sup> and N W Roberts<sup>2</sup>

<sup>1</sup> School of Physics, University of Exeter, Stocker Road, Exeter EX4 4QL, UK

<sup>2</sup> School of Physics and Astronomy, University of Manchester, Manchester M13 9PL, UK

E-mail: [s.a.jewell@exeter.ac.uk](mailto:s.a.jewell@exeter.ac.uk)

*New Journal of Physics* **9** (2007) 99

Received 18 January 2007

Published 23 April 2007

Online at <http://www.njp.org/>

doi:10.1088/1367-2630/9/4/099

**Abstract.** A detailed optical study of the iridescent outer-shell of the beetle *Plusiotis boucardi* has revealed a novel microstructure which controls both the polarization and wavelength of reflected light. A previously unreported hexagonal array across the integument of the beetle exhibits highly localized regions of reflection of only red and green left-handed circularly-polarized light. Optical and transmission electron microscopy (TEM) imaging reveals the origin of this effect as an array of ‘bowl-shaped’ recesses on the elytra that are formed from a dual-pitch helicoidal layer. Reflectivity spectra collected from the beetle are compared to theoretical data produced using a multi-layer optics model for modelling chiral, optically anisotropic media such as cholesteric liquid crystals. Excellent agreement is obtained between data and theory produced using a model that incorporates an upper isotropic layer (of cuticular wax), followed by a short pitch (310 ( $\pm 1$ ) nm) overlying a longer pitch (370 ( $\pm 1$ ) nm) helicoidal layer of optically anisotropic material. These layers are backed by an absorbing underlayer. Synthetic replication of this form of structure may provide a route to the fabrication of tuneable micro-mirrors for optical applications.

<sup>3</sup> Author to whom any correspondence should be addressed.

## Contents

<b>1. Introduction</b>	<b>2</b>
<b>2. Methods and results</b>	<b>3</b>
2.1. Polarization analysis. . . . .	3
2.2. Microscopy studies . . . . .	4
2.3. Spectral analysis. . . . .	7
<b>3. Discussion</b>	<b>7</b>
<b>Acknowledgments</b>	<b>9</b>
<b>References</b>	<b>10</b>

## 1. Introduction

Many members of the *Plusiotis* genus of beetles, native to South America, possess iridescent metallic-looking forewings (elytra). Furthermore, these creatures exhibit the ability selectively to reflect circularly polarized (CP) light, with the vast majority of species reflecting only left-hand CP (LHCP) light (Michelson 1911; Neville and Caveney 1969). In strong contrast to CP light reflected from a plane mirror, which undergoes a  $180^\circ$  phase shift on reflection and changes handedness, the reflected light from the beetle cuticle maintains its original handedness. This conservation of initial handedness is characteristic of the behaviour of CP light interacting with a helicoidal structure composed of anisotropic media whose fast optic-axis rotates with the same handedness as that of the incident light (Dreher and Meier 1973). A common example of this is the reflection of light from a cholesteric liquid crystal structure (Azzam and Bashara 1977) which is composed of partially ordered rod-shaped molecules. Different refractive indices are associated with the short (ordinary) and long (extra-ordinary) molecular axes, denoted by  $n_o$  and  $n_e$  respectively. At all points through the cholesteric structure the long axis lies in a plane perpendicular to the propagation direction of the light (taken to be along the  $z$ -axis) and rotates around the  $z$ -axis through  $360^\circ$  over a distance defined as one pitch.

The elytra of certain *Plusiotis* beetles contain fibrous chitin embedded in a protein matrix (Caveney 1971), with the average azimuthal orientation varying linearly through the layer. This is analogous to the helicoidal microstructure in a cholesteric liquid crystal. The handedness of the reflected light is dictated by the direction of the azimuthal rotation. The peak wavelength of the light reflected,  $\lambda$  is determined by the helicoidal pitch,  $p$ , where

$$\lambda = p\bar{n} \quad (1)$$

and  $\bar{n}$  is the average refractive index of the anisotropic material (De Gennes and Prost 1995).

Recently, interest has arisen in the ability of these helicoidal structures to control the reflection of CP light and the beetle *Plusiotis resplendens* has been used as a blueprint to produce a tuneable optical diode for use in liquid crystal based lasers (Hwang *et al* 2005). Most previous work has concentrated on specific highly metallic-looking silver or gold coloured beetles, with the aim of developing highly efficient reflective surfaces, tuneable to specific wavelengths (Mitov and Dessaud 2006). In this study however, we investigate several beetles (particularly *Plusiotis boucardi*) with green coloured elytra which all selectively reflect CP light.

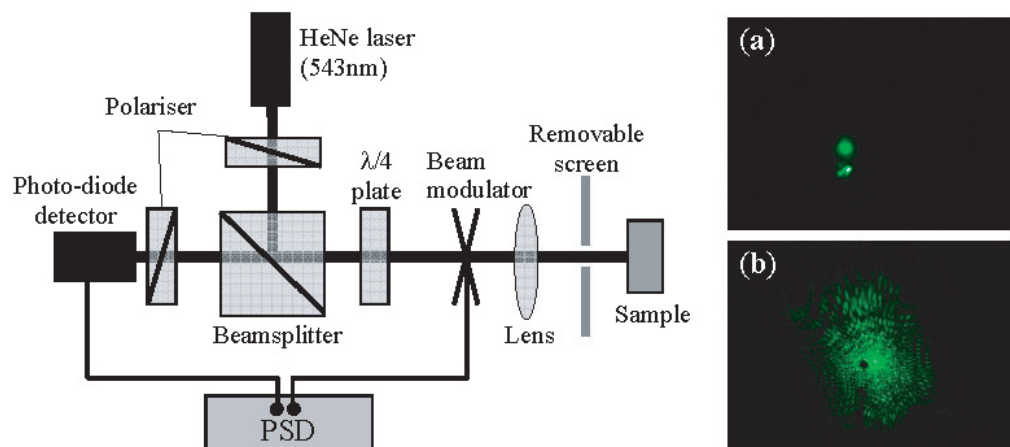


**Figure 1.** Schematic diagram of the technique used to determine selective circular polarization reflectivity from various samples of iridescent beetles. The removable screen was added to allow the scattering of light from (a) *P. resplendens* and (b) *P. boucardi* to be imaged, showing that the light from the second beetle was reflected over a much greater angle range.

## 2. Methods and results

### 2.1. Polarization analysis

To confirm the selective-reflection of CP light and the conservation of CP handedness associated with the interaction of light with chiral structures, the elytra from a selection of beetles were mounted using the experimental set-up shown in figure 1. In this arrangement, light from a 543 nm helium–neon laser passes through a fixed linear polarizer to produce transverse-electric (TE) polarized light. It is then reflected from a 45° beam-splitter and passes through a quarter-wave plate, the axis of which is set to produce either LHCP or right-hand CP (RHCP) light by inducing either a +90° or –90° phase-shift. On reflection from the sample, the light passes back through the quarter-wave plate to then undergo a 90° phase-shift of the opposite sign. Assuming that the light is mainly CP on reflection from the sample it is converted back into linearly polarized light by the quarter-wave plate and hence the total induced phase-shift is zero degrees. This light then passes through the beam-splitter, and the orientation of the linear polarization can be determined using the analysing polarizer on the face of the photodiode detector. To improve the signal-to-noise ratio (SNR), a detector is used in conjunction with a phase sensitive detector (PSD) connected to a beam modulator placed between the quarter-wave plate and sample; in this way, only the light which has been reflected from the sample is recorded. This beam modulation technique is widely used in optical liquid crystal studies (Jewell and Sambles 2003).

Initially, the system was set-up using a plane mirror in place of the sample. When either RHCP light or LHCP light was used, the linearly polarized light arriving at the detector was extinguished when the analyser was set to TE-polarization. This indicated that the initially TE-polarized light had been converted into transverse magnetic (TM)-polarized light, due to the 180° phase-shift produced on reflection from the mirror surface. In contrast to this, when the mirror was replaced with a sample of the *P. boucardi* beetle, a strong signal was detected with the

analyser set to TE-polarized for LHCP. However, negligible light was detected with the analyser set to either TE or TM-polarized when RHCP was used. This confirmed that the *P. boucardi* sample selectively reflected LHCP and that the handedness was conserved on reflection. The process was repeated with several other beetles which were similar in appearance, including *Plusiotis alphabarrerae* and *Plusiotis sallei* and the same result was observed. Interestingly, when a sample of *P. resplendens* was used, a strong signal was detected when both RHCP and LHCP were used. This results from its unique ability to reflect either handedness of light without inducing any phase-shift (Song *et al* 2004).

During this study it was noted that the beetle *P. boucardi* scattered the reflected light over a very wide angle range. Previous studies of the reflection of CP light from the *Plusiotis* genus of beetles have generally concentrated on the highly metallic species such as *P. resplendens* (Hegedüs *et al* 2006). These species tend to scatter reflected light over a much narrower angle range, resulting in an intense reflected spot. Using the set-up shown in figure 1 with the removable screen in place (which had a small hole in the centre to allow the light through) images 1(a) and 1(b) were collected. These show the significant differences in the nature of the reflection. At normal incidence the *P. resplendens* sample reflected the majority of the light back along the same path as the incident beam. However, the reflection from *P. boucardi* was spread over a significantly larger angle range (figure 1(b)). This was also a reason for a significantly lower reflection intensity detected during the CP handedness measurements. The reflected light in this case also appeared to form a regular hexagonal pattern on the plane screen (which was found to be extremely intense when LHCP light was used but very weak for RHCP light) indicating the presence of a hexagonally arranged surface structure.

## 2.2. Microscopy studies

The results of imaging elytra of the *P. boucardi* beetles (figure 2(a)) using an optical microscope in reflection with unpolarized light reveal further details about the structure on the exterior of the elytra. Using bright-field optical microscopy at high magnification a regular structure of close-packed hexagons (diameter  $\approx 10 \mu\text{m}$ ) is observed (figure 2(c)). These have a narrow green border with bright yellow circular centres. The colour of these centres tends towards a weak red at the edges (figure 2(d)). The images shown in figure 2 were obtained from the mid elytral region but this patterning was found to extend over the entirety of the beetle's integument. Figures 2(e) and (f) show the same region as before but in dark-field illumination to highlight the reflection properties of the structure at non-normal incidence. In this case, the distinct hexagonal pattern is still clearly visible but the previously bright centres are black. Additionally, the regions around the core have become intensely bright green in colour.

To observe the *P. boucardi* sample in more detail it was mounted in a confocal microscope with the outer surface of the elytron illuminated at wavelengths of 514 nm (green), 543 nm (green), 594 nm (orange) and 633 nm (red). The images collected indicate that the reflection of the different wavelengths is strongly localized to specific regions of the sample (figure 3). Green light is strongly reflected from both the borders of the hexagons (as previously seen in brightfield illumination) and from their centres. However, red light is only reflected from distinct spots at the centres of the hexagons and perfectly coincides with the positions of the green spots. Orange light was also reflected from these central spots, though with less intensity than the other wavelengths. The combination of the reflected wavelengths at the centre of the hexagons is perceived as yellow. This accounts for the yellow pin-points of light observed under white-light

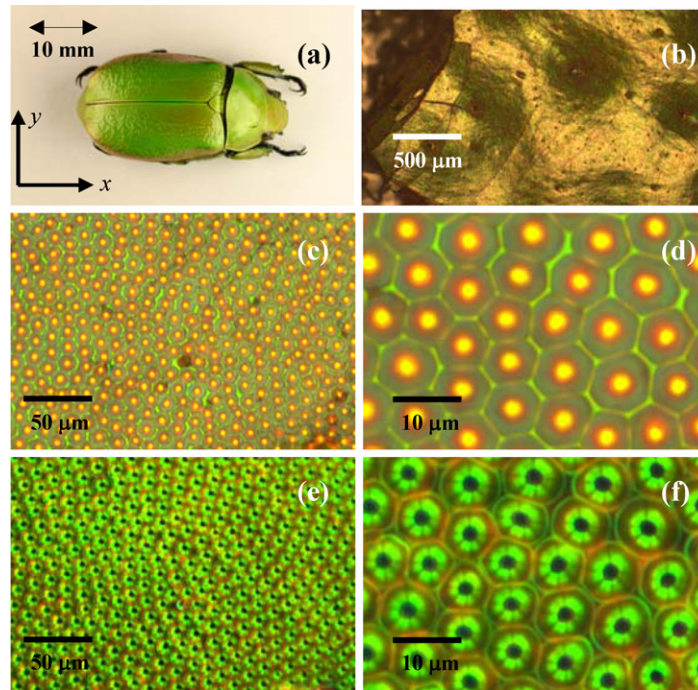


**Figure 2.** (a) Photograph taken of a *P. boucardi* specimen; Images collected from the central region of the back of the beetle using an optical microscope under bright field illumination at magnifications of (b)  $5\times$ , (c)  $20\times$  and (d)  $100\times$ ; images collected under dark-field illumination at magnifications of (e)  $20\times$  and (f)  $100\times$ .

illumination. At each wavelength used with this confocal microscopy there is a distinct contrast between the areas which do and do not reflect the incident light. The annular regions surrounding the central bright spots appear black at all wavelengths (figure 3(a)–(d)), however they were seen to reflect strongly when they were imaged using the microscope in dark-field illumination. This is a further indication that light is reflected over a very wide angle.

To allow a detailed exploration of the underlying structure of the elytra transmission electron microscopy (TEM) images of a cross-section through an elytron of a *P. boucardi* beetle were collected. Figure 4(a) shows a section of *P. boucardi*. The cuticular wax layer is visible as the untextured mid-grey region in the top right of the image and the thick melanin layer is visible in the lower left area. The region between these layers shows distinct structure in the form of shallow, concentrically arced layers below the surface of diameter  $\approx 8\mu\text{m}$ . They correspond closely to the diameter of the hexagons observed under optical microscopy (figure 2(d)). Furthermore, there is an apparently regular packing of the three-dimensional (3D) structures; the layer spacing generally appears smaller in the upper half of the cross-section. However, this is difficult to quantify where the image is in a plane that does not contain the common axis of the concentric bowls. Figure 4(b) was taken at a higher magnification and shows arced formations within each of the layers. This structure is characteristic of a helicoidal structure cut at an oblique angle to the layer normal, and was first observed by Bouligand (1965). Each arc spans one half of the chiral pitch. Although the spacing of the major layers here is  $\approx 300\text{ nm}$  an accurate calculation



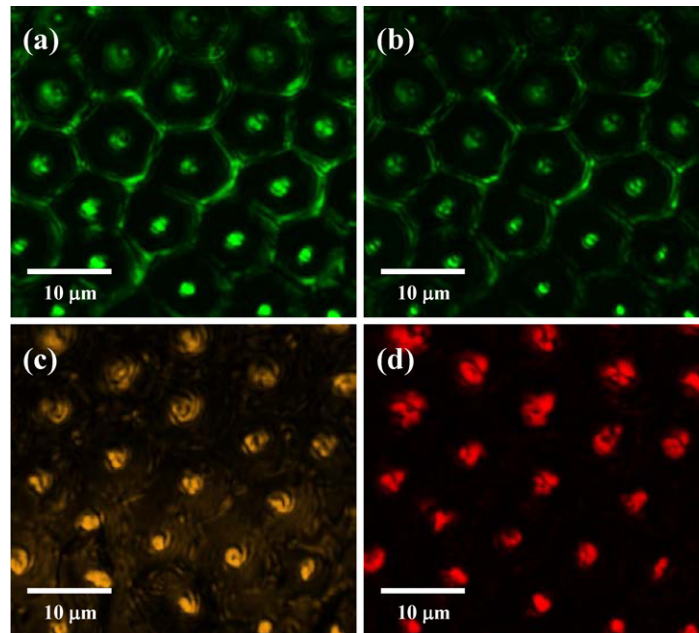


**Figure 3.** Confocal microscope images collected with illumination at (a) 514 nm, (b) 543 nm, (c) 594 nm and (d) 633 nm.

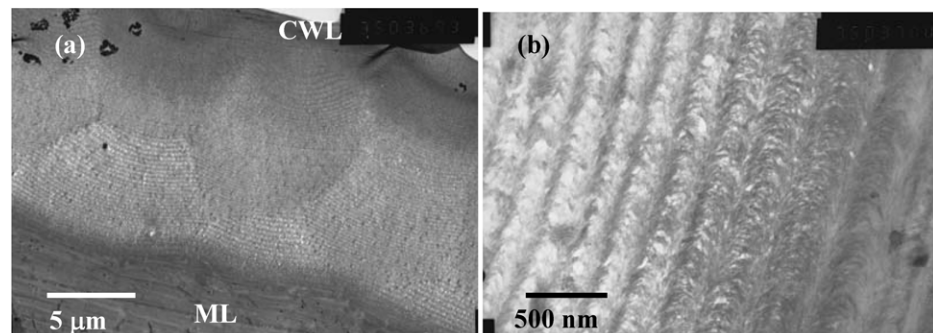


**Figure 4.** TEM images collected from a cross-section through the elytron showing (a) the curved, concentric layering structure observed below the waxy overlayer and (b) Bouligand planes highlighting the helicoidal nature of the layers of fibrous chitin. (CWL, cuticular wax layer; ML, melanin layer.)

of the pitch would require good knowledge of the oblique angle of section, which was difficult to obtain due to the naturally curved and pitted surface of the elytra.

The stacking of curved layers of two different pitches in the underlying structure of *P. boucardi* closely resembles the chiral ‘micro-mirror’ structure seen in the New Zealand Manuka beetle (De Silva 2005). The underlying layers of the Manuka beetle structure clearly exhibit undulating microstructures which appear to be continuous over the elytral surface. This gives rise to fairly randomly sized oval ‘micro-mirrors’. In contrast, *P. boucardi* exhibits a much more regular arrangement of these curved reflecting surfaces in the form of hexagonal ‘cells’ observed at the surface (figure 2(d)). The separation of one cell from another in the underlying media

is far more accurately defined. Furthermore, the pitches associated with the two species differ significantly.

### 2.3. Spectral analysis

Reflection spectra were collected from the sample using the following method. The sample was mounted under the  $5\times$  dry objective of a microscope and an aperture was used to illuminate an area of  $0.07\text{ mm}^2$  with unpolarized light at normal incidence. A polarization insensitive Ocean Optics USB2000 spectrometer was used to analyse the light reflected. A typical reflection spectrum collected from *P. boucardi* is shown in figure 5(a). There are three main peaks, one at 519 nm (green), one at 588 nm (orange) and one at 620 nm (red).

The presence and shape of the strong reflected peaks observed here indicates that two distinctly different pitches are present (see below). This is also implied in the TEM images taken which show the shorter pitch at the top of the stack and the longer pitch below it (figure 4). A further spectroscopic study was performed using the microscope at high magnification with an appropriate pinhole aperture (diameter  $5\text{ }\mu\text{m}$ ). Spectra were collected from points at the centre of one of the hexagonal cells (which appears yellow when viewed through the eyepiece) and from a region where three hexagonal cells intersect (which appears green). As expected, distinct differences were noted in the two spectra. A single peak at the green wavelength was observed in the spectrum collected from the region where the hexagonal cells intersect. In contrast, the spectrum from the centre of a hexagonal cell also showed a peak at red wavelengths. This is in agreement with the images collected using the confocal microscope (figure 3). The tops of the bowl structures are believed to strongly reflect the green light due to the short-pitch layer being uppermost in the sample and the rims of the bowls being normal to the incident ray. As the light propagates further into the material there is an apparent perturbation of the layers in the regions where two bowl structures meet. At these points the periodicity of the longer pitch region is disrupted and is therefore unable to produce the strong red reflection which is seen from the well-defined layers at the centre of the bowls.

## 3. Discussion

The presence of the strong spectral peaks in the reflection from *P. boucardi* confirmed its underlying multiple-pitch chiral system. A simple 1D multi-layer optics model was used to approximate the layers in the beetle elytra and model the reflection from such a planar structure. The model, based on a  $4\times 4$  Berreman matrix (Ko and Sambles 1988) has previously been used to determine wavelength-dependent reflection from stratified liquid crystal layers over a range of angles of incidence (Yang and Sambles 1993; Jewell and Sambles 2006). The 1D model was chosen as a reasonable approximation as light striking the sample at the curved edges of the bowls was reflected off axis, and hence not collected by the spectrometer. Therefore it was assumed that the majority of the light collected was reflected from the edges and bases of the bowl structures (at normal incidence) and hence could be approximated as a multi-layer stack. The basic structure of the 1D multilayer model is shown in figure 5(b) (inset) and comprises a waxy overlayer; a helicoidal region with short-pitch; a helicoidal region with long-pitch and finally a layer of optical absorber. The azimuth (in the  $x$ - $y$ -plane) of the fast-axis of the anisotropic media in the helicoidal layers was assumed to vary linearly as a function of distance through the slab.



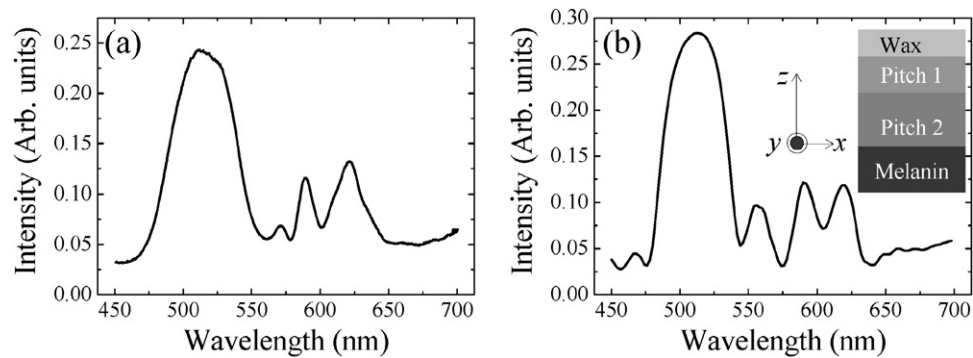


**Figure 5.** (a) Measured reflection spectrum from a sample of the elytron from a *P. boucardi* beetle collected using  $5\times$  magnification and (b) modelled reflection spectrum from a dual-pitch helicoidal structure using the parameters given in the text.

The total rotation angle was determined by the number of pitches of the material used. To calculate the optical properties associated with these layers, each of the two helicoidal slabs (figure 5(b), pitch 1 and pitch 2) were divided into thinner sub-wavelength layers where the orientation of the fast-axis in each layer was assumed to be uniform over the sublayer. It was found that using 25 sublayers per single pitch of the material was sufficient for computational convergence of the theoretical reflection spectra.

No previously published data was available for the optical parameters of the various layers of the elytron for *P. boucardi* so approximations were made using values given in literature for other members of the *Plusiotis* genus (Caveney 1971). Accordingly, for our model both helicoidal regions were assumed to comprise cuticle with refractive indices  $n_{\perp} = 1.70$  and  $n_{\parallel} = 1.58$ . The upper waxy layer was taken as  $n = 1.41$  (Hooper *et al* 2006). For the melanin base layer an isotropic slab with  $n = 2.00$  was used (Land 1972).

The modelling revealed an interesting and unexpected phenomenon. It yielded the expected two strong reflection maxima by way of equation (1), at 519 and 620 nm. Curiously however, it revealed that the origin of the third reflection maxima, at 588 nm, arises from an interference effect produced by the two differently pitched helicoidal regions lying in series with each other. This modelling yielded helicoidal pitches of  $p_1 = 310$  nm and  $p_2 = 370$  nm and will be described later. (It was not possible to obtain the pitch lengths directly from the TEM images collected because the slices were not necessarily cut through the centre of the concentric bowl profiles.) However, the TEM images were in the right range of 300–400 nm for both pitches.

In the modelling the upper helicoidal layer was assigned the shorter pitch, as indicated in the TEM images, with the longer-pitched material directly below it. Additionally, the incident light was assumed to be at normal incidence and a linear combination of TE and TM light (with the reflected light also a linear combination of TE and TM light). The parameters used were fine-tuned to produce theoretical data that showed peak reflection wavelengths which coincided with those measured experimentally. The reflection spectrum produced from this system is shown in figure 5(b). It was modelled using a  $0.75\ \mu\text{m}$  layer of cuticular wax ( $n = 1.41 (\pm 0.01)$ ), two sections of optically anisotropic helicoidal material (both of  $n_o = 1.700 (\pm 0.005)$  and  $n_e = 1.580 (\pm 0.005)$ ) with 9 pitches in the upper region of pitch  $310 (\pm 1)$  nm and 25 pitches in the lower region of  $370 (\pm 1)$  nm. Differences between the measured and modelled reflection

spectra can be attributed to the unknown dispersion of the beetle cuticle as well as the influence of off-axis reflections. Despite the limitations of approximating the structure to a 1D system at normal incidence very good agreement was obtained (see figure 5).

The presence of distinct, well-defined peaks in the reflection spectra of *P. boucardi* is in contrast to the relatively broad range of wavelengths reflected from the more metallic-looking beetles such as *P. optima* and *P. resplendens*. In the latter cases it is feasible that this allows the beetle some form of camouflage through the reflection of its surroundings (Vukusic and Sambles 2003). However, the specific wavelengths reflected from *P. boucardi* suggest that they may be tuned to those wavelengths for a purpose. Spectral matching of visual pigments to an animal's mesopic visual environment is common throughout the animal kingdom and the locations of two of the spectral peaks (519 and 588 nm) may be related to the spectral sensitivity of the beetles. Indeed, several different species of Coleoptera are known to show mid-green wavelength sensitivity (Lin and Wu 1992; Briscoe and Chittka 2001; Dacke *et al* 2002) although the true function of this ability is currently unknown but under investigation. As suggested in recent studies of some Lepidopteran colour (Vukusic and Hooper 2005), it would be an interesting extension to this study to explore the possible link between the reflected spectra and the peak sensitivities of the photoreceptors of conspecifics. Furthermore, many arthropods with similar compound eye designs are known to exhibit sensitivity to polarized light, and nearly always at ultra-violet wavelengths (Frantsevich *et al* 1977; Dacke *et al* 2002, 2003). In the future, it would also be worthwhile investigating possible polarization reflections at UV wavelengths and any connection to the visual ecology of the insect.

The wide-angle reflection of green light incident on the bowl-shaped structures also helps to enhance the beetle's visibility. This property is analogous to the reflection of light from an array of silver spherical concave micro-mirrors of similar dimensions which have been developed for photonic applications (Coyle *et al* 2003). For parallel beams of light incident on the sample, the directions of the reflected rays are dependent on the point on the curved surface on which the beam is incident. This is also generally true for the bowl-shaped recesses on *P. boucardi*'s elytra. In this case, the helicoidal layer adds an additional degree of complexity due to the wavelength dependent reflection.

The mechanism by which the array of the chiral bowls forms on the surface of the beetle is not clearly understood. However, through the use of polymerizable liquid crystals it may be possible to fabricate this structure. The surface tension effects on a sample of cholesteric liquid crystal in contact with a micron-scale mould acting as a template during the evaporation of a host solvent may be sufficient to create these chiral bowl structure arrays. Polymerizing the material into a stable structure would then produce a stable, wavelength-tuned chiral micro-mirror to allow the control of CP light for optical applications.

## Acknowledgments

We thank Professor H F Gleeson of the University of Manchester for the use of the apparatus for the pin-hole microscopy measurements and to acknowledge funding for this project from the BBSRC.

## References

- Azzam R M A and Bashara N M 1977 *Ellipsometry and Polarised Light* (Amsterdam: North Holland)
- Briscoe A D and Chittka L 2001 The evolution of color vision in insects *Annu. Rev. Entomology* **46** 471–510
- Bouligand Y 1965 Sur une architecture torsadée répandue dans la nombreuses cuticules d'arthropodes *C. R. Hebd. Séances. Acad. Sci. Paris* **26** 3665–8
- Caveney S 1971 Cuticle reflectivity and optical activity in scarab beetles: the role of uric acid *Proc. R. Soc. Lond. B* **178** 205–25
- Coyle S, Prakash G V, Baumberg J J, Abdalsalem M and Bartlett P N 2003 Spherical micromirrors from templated self-assembly: Polarization rotation on the micron scale *Appl. Phys. Lett.* **83** 767–9
- Dacke M, Nordström P, Scholtz C H and Warrant E J 2002 A specialized dorsal rim area for polarized detection in the compound eye of the scarab beetle *Pachysoma striatum* *J. Comp. Physiol. A* **188** 211–6
- Dacke M, Nilsson D E, Scholtz C H, Byrne M and Warrant E J 2003 Insect orientation to polarized moonlight *Nature* **424** 33
- De Gennes P G and Prost J 1995 *The Physics of Liquid Crystals* (Oxford: Oxford University Press)
- De Silva L, Hodgkinson I, Murray P, Wu Q H, Arnols M, Leader J and McNaughton A 2005 Natural and nanoengineered chiral reflectors: structural colour of Manuka beetles and titania coatings *Electromagnetics* **25** 391–408
- Dreher R and Meier G 1973 Optical properties of cholesterics *Phys. Rev. A* **8** 1616–23
- Frantsevich L, Govardovski V, Gribakin F, Nikolajev G, Pichka V, Polanovsky A, Shevchenko V and Zolotov V 1977 Astro-orientation in *Lethrus* (Coleoptera, Scarabaeidae) *J. Comp. Physiol.* **121** 253–71
- Hegedüs R, Szél G and Horváth G 2006 Imaging polarimetry of the circularly polarizing cuticle of scarab beetles (Coleoptera: Rutelidae, Cetoniidae) *Vision Res.* **46** 2786–97
- Hooper I R, Vukusic P and Wootton R J 2006 Detailed optical study of the transparent wing membranes of the dragonfly *Aeshna cyanea* *Opt. Express* **14** 4891–7
- Hwang J, Song M H, Park B, Nishimura S, Toyooka T, Wu J W, Takanishi Y, Ishikawa K and Takezoe H 2005 Electro-tuneable optical diode based on photonic bandgap liquid-crystal heterojunctions *Nat. Mater.* **4** 383–7
- Jewell S A and Sambles J R 2003 Fully-leaky guided mode measurement of the flexoelectric constant ( $e_{11} + e_{33}$ ) of a nematic liquid crystal *Mol. Cryst. Liq. Cryst.* **401** 181
- Jewell S A and Sambles J R 2006 Dynamic response of a dual-frequency chiral hybrid aligned nematic liquid crystal cell *Phys. Rev. E* **73** 011706
- Ko D Y K and Sambles J R 1988 Scattering matrix method for propagation in stratified media *J. Opt. Soc. Am. A* **5** 1863–6
- Land M F 1972 The physics and biology of animal reflectors *Prog. Biophys. Mol. Biol.* **25** 75–106
- Lin J T and Wu C Y 1992 A comparative-study on the color-vision of 4 coleopteran insects *Bull. Inst. Zool., Acad. Sin.* **31** 81–8
- Michelson A A 1911 On metallic colouring in birds and insects *Phil. Mag.* **21** 554–67
- Mitov M and Dessaud N 2006 Going beyond the reflectance limit of cholesteric liquid crystals *Nat. Mater.* **5** 361–4
- Neville A C and Caveney S 1969 Scarabeid beetle exocuticle as an optical analogue of cholesteric liquid crystals *Biol. Rev.* **44** 531–62
- Song M H *et al* 2004 Effect of phase retardation on defect mode lasing in polymeric cholesteric liquid crystals *Adv. Mater.* **16** 9–10
- Vukusic P and Hooper I 2005 Directionally controlled fluorescence emission in butterflies *Science* **310** 1151
- Vukusic P and Sambles J R 2003 Photonic structures in biology *Nature* **424** 852–5
- Yang F and Sambles J R 1993 Optical characterisation of liquid crystals by means of half-leaky guided modes *J. Opt. Soc. Am. B* **10** 858–66